Preprint of a paper which appeared in
Proceedings of the International Conference on Process Machine Interactions,
pp. 223-230, 3-4 September, 2008

Prediction of the Tool Displacement by Coupled Models of the Compliant Industrial Robot and the Milling Process

E. Abele[1], J. Bauer[1], S. Rothenbücher[1], M. Stelzer[2], O. von Stryk[2]
Technische Universität Darmstadt, Germany
[1]Institute of Production Management, Technology and Machine Tools (PTW)
[2]Simulation, Systems Optimization and Robotics Group (SIM)
bauer@ptw.tu-darmstadt.de
stelzer@sim.tu-darmstadt.de

Abstract
Using an industrial robot for machining parts provides a cost-saving and flexible alternative to machine tools. However, reachable accuracies are often insufficient due to the lower stiffness of the robot structure. This paper presents a method to predict the displacement of the tool by coupling the elastic serial robot model with the milling process model. For this a common process model is used to estimate the process force in a high compliant serial robot structure. Based on experimental results the validity of the process model due to the high compliance is investigated.

Keywords
Process Machine Interaction, Milling Process, Robot Structure

1 INTRODUCTION

The major field of cutting applications for industrial robots is automated pre-machining (deburring and fettling) of cast parts. There, industrial robots substitute manual work under rough conditions and in some cases even expensive five axis machine tools. A new economic opportunity would be to use the robot also for middle tolerance end-milling. However, through the compliant serial robot structure the non constant process forces cause a static displacement and an excitation of the robot eigenfrequencies, which lead to low frequency oscillations of the tool tip. Hence, especially at high metal removal rates and high feed rates the achievable accuracy is limited and often insufficient.

This article discusses a method to predict the static displacement as well as low frequency oscillations of the tool tip by coupling a robot model with a milling process model. In chapter 2 experimental studies show the differences between the milling operation on a standard three axis milling machine and the industrial robot. Additionally, effects of the robot milling operations which have to be considered in modeling the mechanical structure of the robot and the milling process are discussed. In chapter 3 the modeling of the robot and the process are examined. In order to obtain a high accurate robot model significant research was done at PTW within in the last years [1,2,8]. A close to reality model behavior can be obtained with a so called virtual joint approach. This method introduces another two (virtual) degrees of freedom per robot axis to describe not only the gears elasticity but also the link deformations and the bearings tipping in the orthogonal axis directions. The prediction of the cutting forces is done with a standard cutting force model based on Altintas [3,4]. By coupling this model to the robot model the Cartesian displacement of the tool path can be computed. In a further step the predicted Cartesian displacements can be used for an error-adapted trajectory generation to improve the static accuracy of milling industrial robots.

2 MEASUREMENTS

The influence of the compliant robot structure on the milling process and the milling force is analyzed with two experimental tests on two different machine types. In both tests the milling operation is full slotting (a_p = 1 mm) of a linear path in Aluminum 3.1325 with a two flute end mill of d = 16 mm. The feed rate in all tests is v_F = 100 mm/s. The spindle being used is a highspeed synchronous spindle achieving a maximum revolution of n = 40.000 min^{-1} and a maximum power of 4.3 kW (S1) with a HSK 32 interface. The spindle speed in the tests is n = 10.000 min^{-1} which is measured with an internal speed and position sensor. During the milling operation the process forces are measured with a Kistler dynamometer of type 9257A.

2.1 Milling Machine

In this setup the spindle is mounted on a standard five axis milling machine. Figure 1 shows the experimental setup for the cutting operation. The feed direction is in positive x.

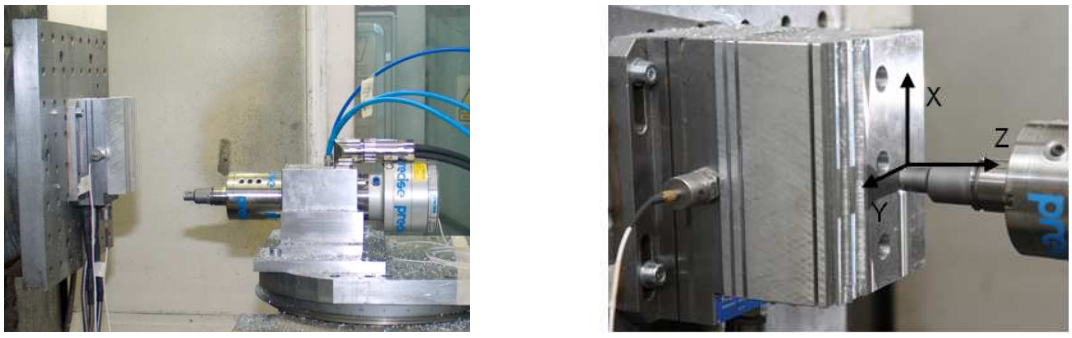

Figure 1: Milling experiment – Standard milling machine

The measured forces which are acting at the tool centre point (TCP) are shown in figure 2. To observe the static force components the force signals are filtered with a cut off frequency of f_c = 200Hz. With these new signals $F_{y,stat}$ and $F_{z,stat}$ also low frequent components that may result from the mechanical structure can be investigated. Both forces show a constant static force level with $F_{y,stat}$ = 120 N and $F_{z,stat}$ = 50 N. Due to the stiffness of the machine tool structure no low frequent oscillations are present in the static force signal.

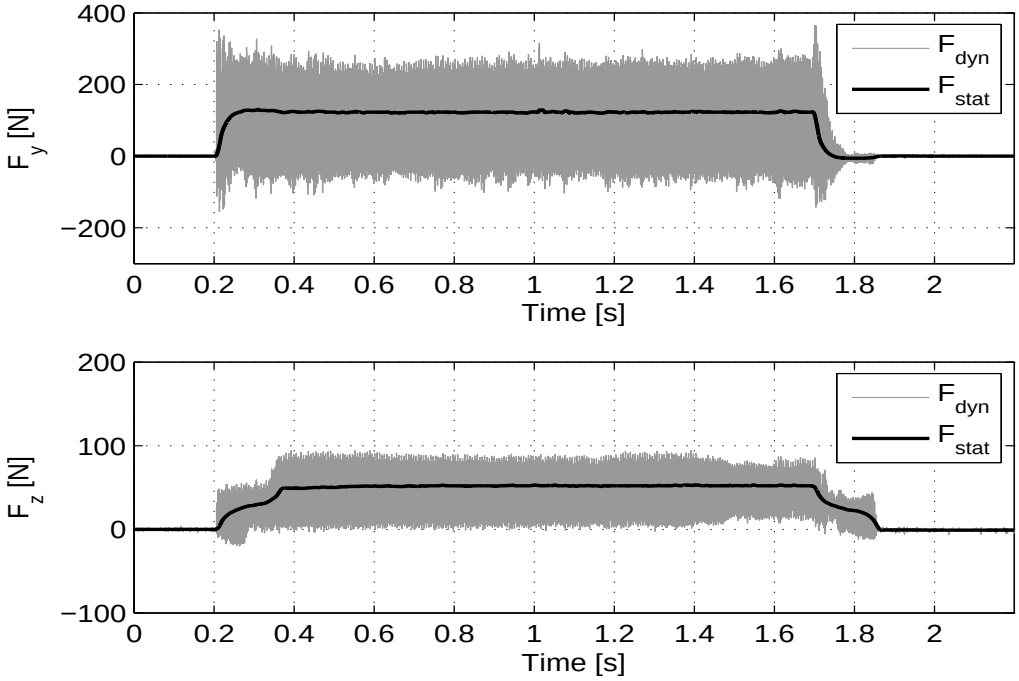

Figure 2: Force Measurement

2.2 Industrial Robot

In this test case the spindle is mounted on the robot. In addition two sensors are added on the spindle to measure the distance between the spindle and the reference bar in y- and z-direction.

The CCD laser displacement sensors are of the type KEYENCE LK-G32. The reference bar is a prismatic guide with a high accuracy of straightness. To avoid any distortion of straightness or vibration of the bar it is just laid on the support and not directly connected to the work piece.

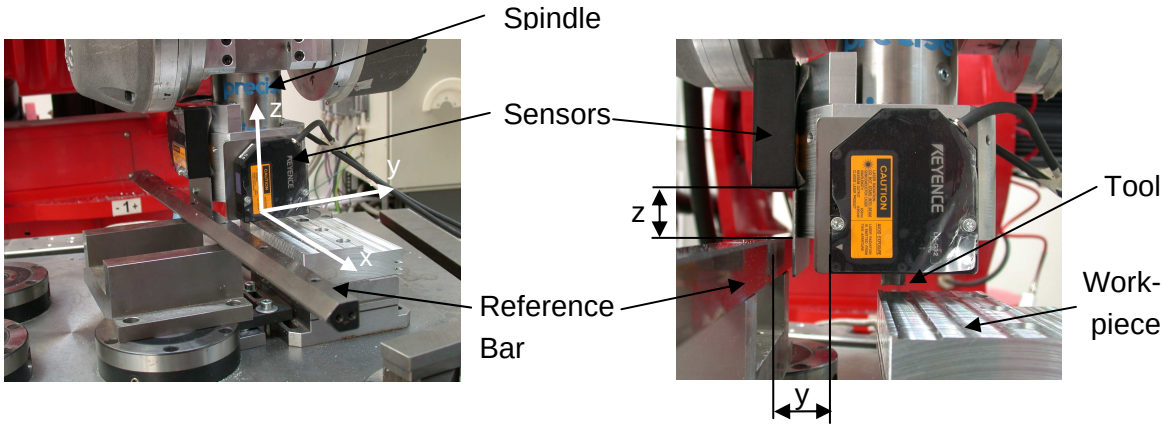

Figure 3: Measurement of the TCP displacement

Conducting the test with the described settings the process forces F_y, F_z and the displacements y, z of the tool centre point (TCP) of the robot are measured and displayed in Figure 4.

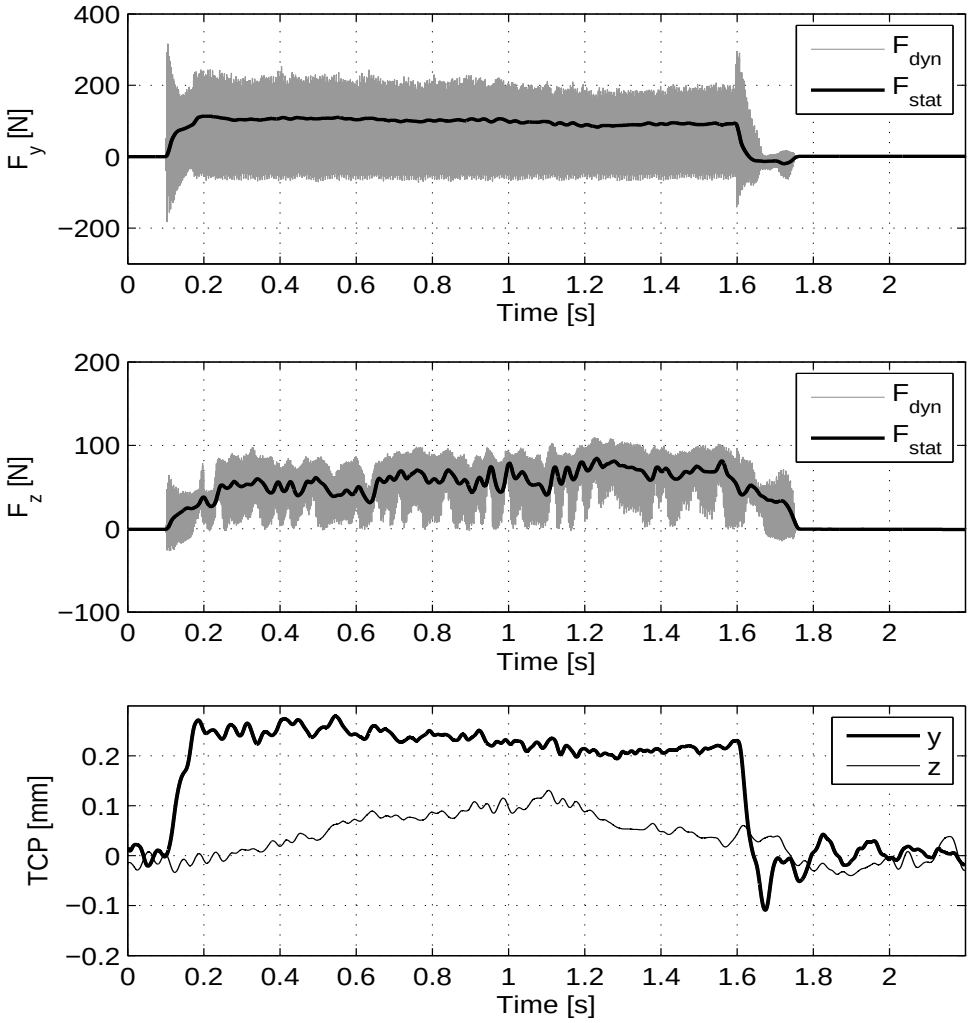

Figure 4: Milling with the industrial robot at n = 10.000 min^{-1}

At the beginning of the cutting operation at t = 0.1 s the TCP trajectory of the robot displaces approximately 0.25 mm in y- and max. 0.1 mm in z-direction due to the cutting forces. While the TCP in y displaces immediately as the cut begins the z displacement increases slowly. This

mechanical behavior of the structure in z- direction can currently not be explained in detail. It is assumed that the z displacement is influenced by the integrated gravity compensation of the robot which causes a high damping of the mechanical structure. Considering the TCP path of the y displacement, an increase of y is expected due to the path of the milling operation under the theoretical condition of constant force. This would occur because on the path of the operation the robot moves from a mechanical stiffer position into a less stiff position within the working space. However, the y path of the TCP shows a decreasing movement. This can be explained by the movement of the TCP in positive z-direction up to 0.1 mm. The cutter experiences a reducing axial depth of cut a_p until it reaches t = 1.1 s which causes a smaller cutting force F_y and hence an decrease of the TCP displacement in y.

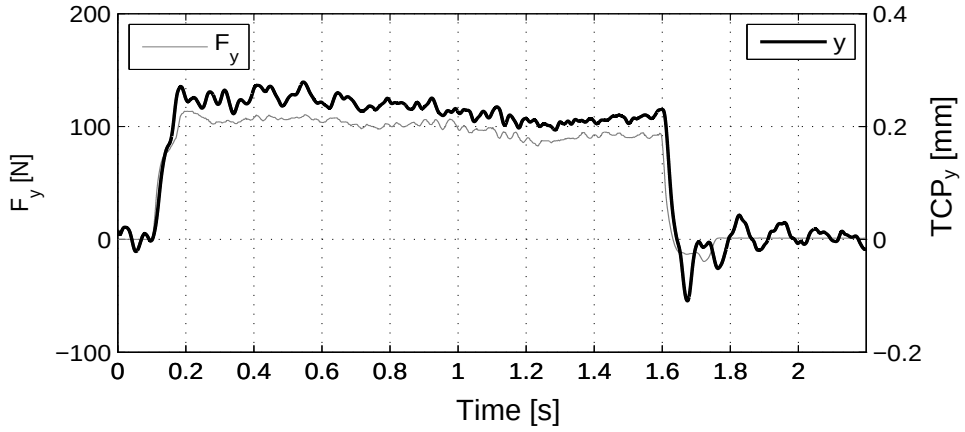

Figure 5: Comparison of force $F_{y,stat}$ and TCP displacement y

In figure 5 the comparison of the low frequency oscillations in the static force signal $F_{y,stat}$ and the TCP displacement y is displayed. Both signals show a direct relationship regarding the distortions. This means that the process force has a direct influence on the amount of TCP displacement. The oscillation between t = 0.2 – 0.7 s and t = 1.6 – 2.1 s are dominated by the excitation of the Eigenfrequency at f = 8.5 Hz of the compliant mechanical structure when the cutter enters and exits the work piece. The oscillation at the work piece entry does not show a free oscillation since it is influenced by the cutting process of the full slotting operation. A free oscillation of the robot is measured between t = 1.6 s and t = 2.1 s since the tool is already outside the work piece. The spectral analysis of both decaying oscillations reveals a slight increase of the frequencies, which points to some kind of nonlinear effect. Additional oscillations of an amplitude about y = ± 0.04 mm can be observed between t = 0.8 to 1.6 s which is found on the work piece surface. It is assumed that this effect is caused by the cutting process and machine interaction since the distortion can be observed to some extend in the force signal as well (see Figure 5). Finally, a trajectory inaccuracy of the serial machine concept without the cutting process of within ±0.02 mm due to the rotational axes and gears is measured.

2.3 Conclusion of the experiments

The two different experiments show that the static forces during the milling operation of the industrial robot ($F_{y,Robot}$ = 100 N, $F_{z,Robot}$ = 55 N) and the forces at standard machine tool ($F_{y,MTool}$ = 120 N, $F_{z,Mtool}$ = 50 N) have nearly equal force level (cf. Figure 6). However, the robot force signal especially in z- direction shows strong distortions over the cutting operation compared to the machine tool force signal.

The unsteady force level in $F_{z,stat}$ affects the displacement of the TCP by an amplitude of z = ±0.03 mm (cf. Figure 4), which finally causes a wavy surface on the work piece. It is observed, that the static process force displaces the TCP trajectory due to the low stiffness of the robot structure up to 0.25 mm in y-direction and 0.1 mm in z-direction, which is the major disadvantage in milling with industrial robots.

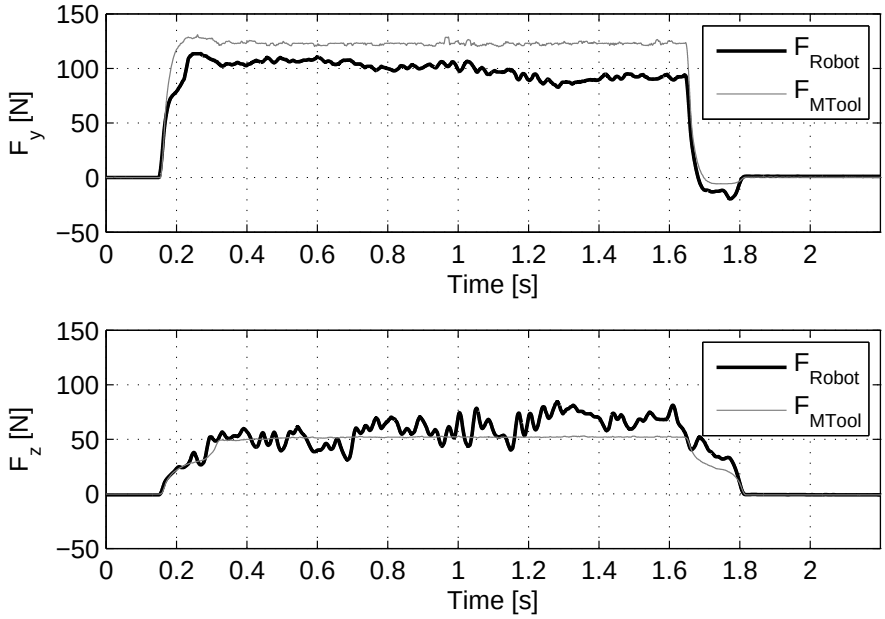

Figure 6: Static forces F_v, F_z of the robot and the machine tool cutting operation

3 MODEL

3.1 Robot Model

In order to simulate the dynamics of the mechanical robot structure a serial multibody model with rigid arm parts and joint elasticities in rotational directions is built in Matlab/ SimMechanics based on the following equations [6,7]

$$\begin{aligned} \mathbf{M}(\mathbf{q})\ddot{\mathbf{q}} + \mathbf{C}(\mathbf{q},\dot{\mathbf{q}}) + \mathbf{G}(\mathbf{q}) &= \tau + \mathbf{S}(\mathbf{F}_{xyz},\mathbf{q}) \\ \mathbf{K}_r(\boldsymbol{\Theta} - \mathbf{q}_r) &= \tau \end{aligned} \quad . \tag{1}$$

The model consists of five rigid bodies and r=5 rotational axes q_r. Since the real robot structure shows compliances orthogonal to the rotational axis additional v = 6 virtual axis q_v and virtual elasticities $\mathbf{K}_v$ are integrated (cf. Figure 7) [2]. The model consists of m = r + v degrees of freedom and is described by the mass/ inertia matrix $\mathbf{M} \in \Re^{m \times m}$, the coriolis/ centrifugal forces $\mathbf{C} \in \Re^{m}$ and the gravitational forces $\mathbf{G} \in \Re^{m}$. The input of the robot model is the vector of joint angles $\boldsymbol{\Theta} \in \Re^{r}$ of the five real axes recorded during the experimental cutting operation. Subtracting $\boldsymbol{\Theta}$ from the axle position $\mathbf{q}_r \in \Re^{r}$ and multiplying the difference with the stiffness matrix $\mathbf{K}_r \in \Re^{r}$ results in the torque $\tau \in \Re^{r}$ applied to the rigid bodies. Using the experimentally measured $\boldsymbol{\Theta}$ as model input the calculated TCP trajectory and the measured trajectory can directly be compared, without the influence of the trajectory planning and interpolation of the robot control.

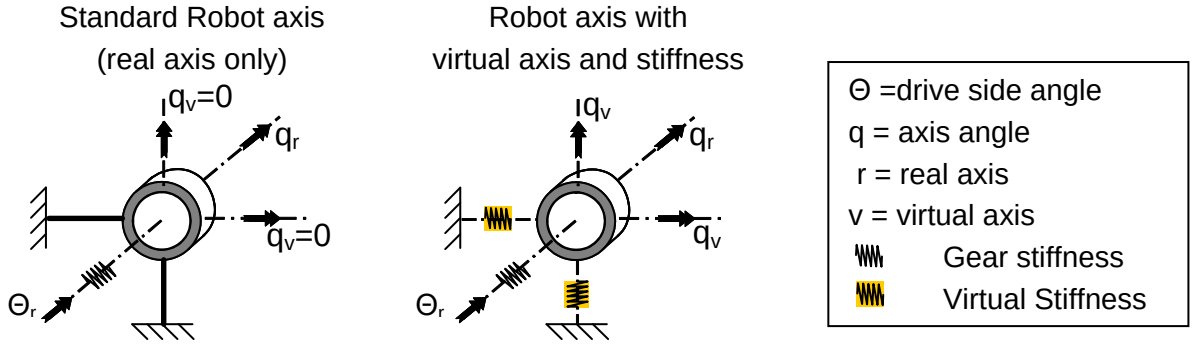

Figure 7: Modeling of the robot axis

The experimental determination of the stiffnesses and the masses of the arm parts is carried out in [8]. It is shown, that the Cartesian stiffness of the robot at the TCP varies strongly over the working area.

3.2 Process Model

Predicting the cutting forces, a standard cutting force model Eq. 2 from Altintas [1,2] is used.

$$\mathbf{F}_{rta,j}(t) = \mathbf{K}_c a_p h_j(t, t-\tau) + \mathbf{K}_e a_p \tag{2}$$

Here, $\mathbf{F}_{rta,j}$ represents the radial, tangential and axial forces per tooth j. These forces are calculated with the specific cutting force $\mathbf{K}_c = [K_{rc}, K_{tc}, K_{ac}]^T$, the axial depth of cut a_p, the chip thickness h_j and the edge forces $\mathbf{K}_e = [K_{re}, K_{te}, K_{ae}]^T$. The chip thickness consists of a static part h_{stat} and a dynamic part h_{dyn}. The static part describes the thickness according to the feed rate f_z with $h_{stat} = f_z \sin(\varphi_j(t))$. The angle φ_j of the teeth j can be calculated with

$$\varphi_j(t) = \varphi(t) + j \cdot 2\pi / N_z \qquad \text{with} \qquad \varphi(t) = \frac{2\pi n}{60} t \tag{3}$$

where N_z being the number of teeth and n the spindle speed in min^{-1}. The dynamic chip thickness is dependent on the actual position of the cutting tooth $\mathbf{u}(t) = [x(t), y(t)]^T$ and the position of the previous tooth $\mathbf{u}(t-\tau) = [x(t-\tau), y(t-\tau)]^T$. The complete equation of the chip thickness can be formulated as

$$h_j(t, t-\tau) = f_z \sin(\varphi_j(t)) + [\sin(\varphi_j(t)) \quad \cos(\varphi_j(t))][\mathbf{u}(t) - \mathbf{u}(t-\tau)]. \tag{4}$$

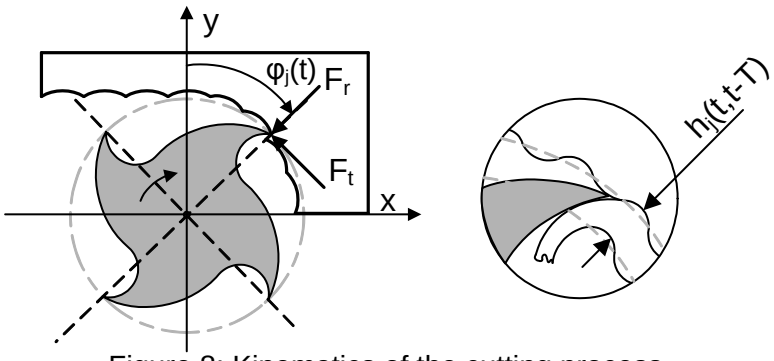

Figure 8: Kinematics of the cutting process

By transforming Eq.2 with the matrix $T_j(\varphi_j)$ and summing over the number of teeth

$$\mathbf{F}_{xyz}(t) = \sum_{j=1}^{N_z} g_j(\varphi_j) \cdot \mathbf{T}_j(\varphi_j) \cdot \mathbf{F}_{rta,j}(t) \qquad \text{with} \qquad \mathbf{T}_j(\varphi_j) = \begin{bmatrix} -\sin(\varphi_j(t)) & -\cos(\varphi_j(t)) & 0 \\ -\cos(\varphi_j(t)) & \sin(\varphi_j(t)) & 0 \\ 0 & 0 & 1 \end{bmatrix} \tag{5}$$

the force F_{xyz} in Cartesian space is calculated. In order to sum only the cutting forces of those teeth which are currently in contact with the material the function $g_j(\varphi_j)$ returns a constant factor 1 for the case of material contact and 0 for outside of the material for the corresponding tooth j. The process model itself is validated through experiments on a milling machine. In different test rows the milling coefficients could be determined by a linear recursion as described in [5]. Since the main focus is the implementation of the process model in a compliant structure the static component of the process force is important.

3.3 Coupling the Robot and the Process Model

The coupling of both models is built completely within the Matlab environment. The Cartesian process force, calculated with the cutting force model of eq.5, is the input for the TCP load in the structural model. The resulting displacement of the TCP is returned into the cutting force model for calculating the dynamic chip thickness and the resulting forces. The overall simulation parameters now depend on the fastest process, which is the calculation of the cutting forces.

Figure 9 shows the measured (y_{Mea}, z_{Mea}) and the simulated (y_{Sim}, z_{Sim}) displacement of the TCP of the coupled process simulation.

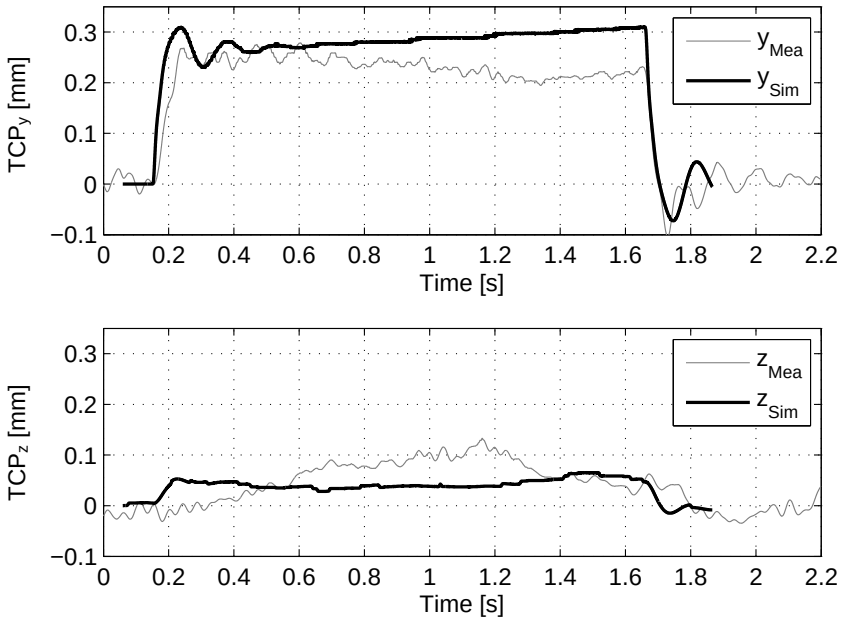

Figure 9: Simulation of the TCP displacement in y and z

Based on the calculated cutting forces the simulated TCP trajectory displaces by y = 0.25 – 0.3 mm and z = 0.06 mm. In comparison with the measurement, the simulation shows a similar static level of displacement in y. However, an increasing force due to the change of mechanical stiffness from the start to the end position within the moving path cannot be verified by the measurement in this extend. In z the simulated results are not comparable for the reasons discussed in chapter 2.2. In contrast to the measured displacement in y, the immediately applied forces cause a simulated overshooting at t = 0.2 s which is not limited by the cutting operation. Within the time span of t = 0.8 – 1.6 s the simulation does not show major distortions of the TCP trajectory, while the measurement contains oscillations due to the cutting forces and hence due to the machine-process interaction. This means that the dynamic process force, modeled by the contact condition of a tool tooth and the dynamic chip thickness h_{dyn}, which both should excite the mechanism of the process-machine interaction only shows a small effect in the TCP trajectory simulation. The reason is the high spindle speed, which excites the mechanical robot system above the first eigenfrequencies in an overcritical area of frequency. Furthermore, the high spindle speed evokes only a small variation of h_{dyn} and hence a minimal variation of the process force. Since the measurements show a continuing oscillation during the operation a revised process force model has to be implemented. Considering the high spindle speed the low frequent oscillation of the TCP can be interpreted as steady change of the milling direction and therefore the direction of the milling forces. The current process model calculates the amount of force due to the TCP displacement. However the direction of the calculated forces is constant. Therefore, in the adapted cutting force model the direction of the cutting forces in respect to the TCP oscillation has to be calculated.

4 SUMMARY AND OUTLOOK

The machining experiments demonstrated that the static level of the process force $F_{y,stat}$ and $F_{z,stat}$ nearly have the same magnitude during the machine tool and the robot operation. Due to the robot compliance the induced static path displacement is one of the major problems in robotic machining. Beside this, the low frequent oscillations are present in F_{stat} and in the TCP displacement of the robot trajectory caused by the excited Eigenfrequency and process - machine interaction which affects the surface quality.

In order to model the displacement of the TCP trajectory, a dynamic model of the robot and a cutting force model are set up. While the static displacements in y are comparable the z component does not match due to the unexpected robot movement in z. The large oscillation

at the beginning and outside of the cutting operation seems to have a lack of damping. Hence the identification of the damping parameters for the robot model is going to be investigated on different points in the working space. Considering the machining operation, the process machine interaction is not present in the simulation in form of excited Eigenfrequencies and oscillations except at the start of the cut. For this reason a refined cutting force model will be implemented which considers the current TCP oscillation to the force direction. Additionally, in the next mechanical model of the robot nonlinear stiffness and loose is considered.

5 REFERENCES

[1] Abele E., Weigold M., Rothenbücher S., 2007, Modeling and Identification of an Industrial Robot for Machining Applications. Annals of the CIRP Vol. 56/1/2007: p. 387

[2] Abele E., Rothenbücher S., Weigold M., 2008, Cartesian Compliance Model for Industrial Robots using Virtual Joints. Production Engineering (tba)

[3] Altintas, Y., 2000, Modelling Approaches and Software for Predicting the Performance of Milling Operations at MAL – UBC, Proceedings of the Third CIRP International Workshop on Modelling of Machining Operations, Sydney, Australia, 2000, pp. 60–74.

[4] Altintas Y., 2000, Manufacturing Automation: Metal Cutting Mechanics, Machine Tool Vibrations, and CNC Design, Cambridge University Press

[5] Gradisek, J., Kalveram, M., Weinert, K., 2004, Mechanistic identification of specific force coefficients for a general end mill, International Journal of Machine Tools and Manufacture 44, S. 401-414

[6] Hölzl, J., 1993, Modellierung, Identifikation und Simulation der Dynamik von Industrierobotern, Dissertation, TU München

[7] Sciavicco, S., Siciliano, B., 1996, Modeling and Control of Robot Manipulators, McGraw-Hill Companies

[8] Weigold, M., 2008, Kompensation der Werkzeugabdrängung bei der spanenden Bearbeitung mit Industrierobotern, Dissertation, TU Darmstadt